

A newly discovered PD-L1 B-cell epitope peptide vaccine (PDL1-Vaxx) exhibits potent immune responses and effective anti-tumor immunity in multiple syngeneic mice models and (synergizes) in combination with a dual HER-2 B-cell vaccine (B-Vaxx)

Linlin Guo^a, Jay Overholser^a, Heather Darby^b, Nicholas J. Ede^c, and Pravin T.P. Kaumaya^{id a,d}

^aDepartment of Obstetrics & Gynecology, The Ohio State University Wexner Medical Center, USA; ^bLicensing Technology, Luminex Corp, Austin Texas, USA; ^cImugene Ltd, Sydney, Australia; ^dThe James Comprehensive Cancer Center, Columbus, OH, USA

ABSTRACT

Blockade of checkpoint receptors with monoclonal antibodies against CTLA-4, PD-1 and PD-L1 has shown great clinical success in several cancer subtypes, yielding unprecedented responses albeit a significant number of patients develop resistance and remain refractory. Both PD-1/PD-L1 and HER-2 signaling pathway inhibitors have limited efficacy and exhibits significant toxicities that limit their use. Ongoing clinical studies support the need for rationale combination of immuno-oncology agents to make a significant impact in the lives of cancer patients. We introduce the development of a novel chimeric PD-L1 B-cell peptide epitope vaccine (amino acid 130–147) linked to a “promiscuous” T cell measles virus fusion (MVF) peptide (MVF-PD-L1(130); PDL1-Vaxx) or linked to tetanus toxoid (TT3) TT3-PD-L1 (130) via a linker (GPSL). These vaccine constructs are highly immunogenic and antigenic in several syngeneic animal models. The PD-L1 vaccines elicited high titers of polyclonal antibodies that inhibit tumor growth in multiple syngeneic cancer models, eliciting antibodies of different subtypes IgG1, IgG2a, IgG2b and IgG3, induced PD-1/PD-L1 blockade, decreased proliferation, induced apoptosis and caused ADCC of tumor cells. The PDL1-Vaxx induces similar inhibition of tumor growth versus the standard anti-mouse PD-L1 antibody in both syngeneic BALB/c and C57BL/6J mouse models. The combination of PDL1-Vaxx with HER-2 vaccine B-Vaxx demonstrated synergistic tumor inhibition in D2F2/E2 carcinoma cell line. The anti-PDL1-Vaxx block PD-1/PD-L1 interaction and significantly prolonged anti-tumor responses in multiple syngeneic tumor models. The combination of HER-2 vaccine (B-Vaxx) with either PDL1-Vaxx or PD1-Vaxx demonstrated synergistic tumor inhibition. PDL1-Vaxx is a promising novel safe checkpoint inhibitor vaccine.

ARTICLE HISTORY

Received 2 August 2022
Revised 15 September 2022
Accepted 15 September 2022

KEYWORDS

B-cell epitope; CT26; D2F2/E2; immunotherapy; PD-L1; Peptide-vaccine

Introduction

The advent of immune checkpoint inhibitors launched a novel era in immunotherapy of cancer. Blockade of program cell death protein 1 (PD-1), programmed death ligand 1 (PD-L1) and cytotoxic T-lymphocyte-associated protein 4 (CTLA-4) with monoclonal antibodies (mAbs) has shown impressive clinical outcomes and superior antitumor activity in patients with different malignancies.^{1–5} PD-1 together with its two ligands PD-L1 and PD-L2 play key roles in regulating the immune system. PD-1 is expressed on activated T-cell, B-cell and myeloid cells,^{6,7} whereas PD-L1 (B7-H1) is largely expressed on multiple tumors including ovarian, non-small-cell lung cancer and melanoma.^{8,9} The engagement of PD-1 by PD-L1 will inhibit T-cell proliferation and cytokines secretion.¹⁰ The blockade of PD-1/PD-L1 interaction is one of the main strategies in the fight against human cancers.

There are currently several FDA approved mAbs targeting PD-1 Opdivo® (Nivolumab), Keytruda® (Pembrolizumab) and PD-L1 Tecentriq® (Atezolizumab), Bavencio® (Avelumab) and Imfinzi® (Durvalumab) as well as several ongoing clinical trials of checkpoint inhibitors in multiple tumor types which have

enabled the development of breakthrough therapies in oncology. These mAb treatments when used as monotherapy have shown significant clinical benefit albeit with significant shortcomings such as low response rates (15–20%),¹¹ toxicity problems, resistance, high costs or financial toxicity, sophisticated therapeutic regimens and long half-life are important impediments that require new and innovative strategies. Furthermore, overcoming these limitations will either necessitate the development of more effective immune checkpoint inhibitors or require innovative combinatorial strategies.

We have advanced the idea of using active immunotherapy with chimeric B-cell epitope peptides incorporating a ‘promiscuous’ T-cell epitope that elicits a polyclonal antibody response which provide safe, cost-effective therapeutic advantage over mAbs. We recently developed a PD-1 B-cell epitope peptide vaccine (PD1-Vaxx; MVF-PD-1(92–110) which outperformed the standard anti-mouse PD-1 antibody (clone 29F.1A12)) in a mouse model of colon carcinoma expressing human HER-2.¹² Additionally, we determined that the combination of PD1-Vaxx with dual HER-2 peptide vaccine (B-Vaxx),^{13–15} showed significant enhanced inhibition of tumor growth in colon carcinoma

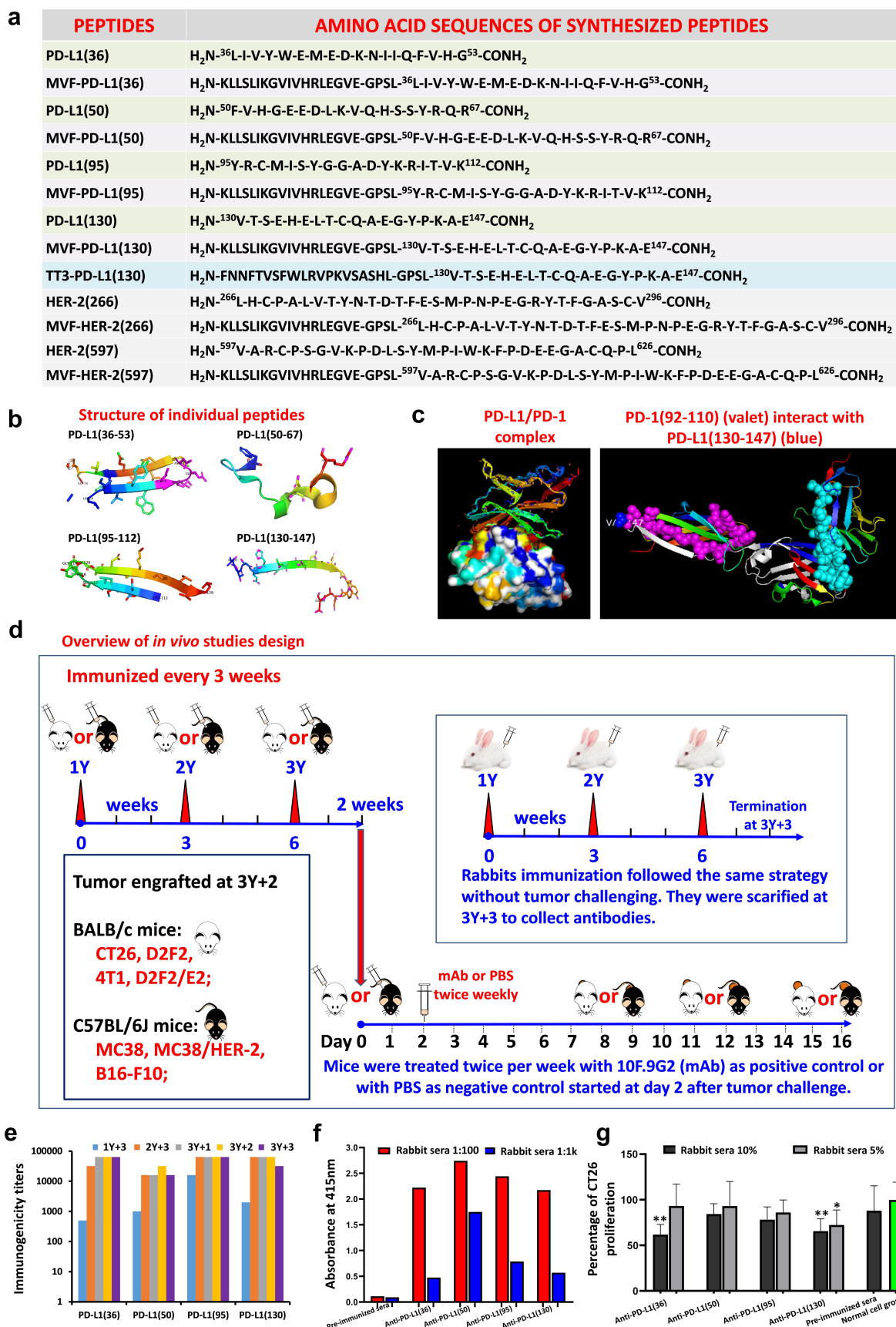


Figure 1. Identification of four B-cell epitope sequences of human PD-L1. (a): Amino acid sequences of human PD-L1. The PD-L1 epitopes of 36–53, 50–67, 95–112 and 130–147 peptides were chosen for investigation. HER-2 or MVF-HER-2 and TT3 sequences are depicted in the table. Briefly, the PD-L1 sequences were subjected to several computerized algorithms that predicts location of epitopes that are surface oriented, have high hydrophilicity, flexibility/mobility, exposure, protrusion and high antigenicity values. The best scoring epitopes are then idealized by correlation with known crystal structures of PD-L1(3BIS) (4Z18), complexes of PD-1:PD-L1(3BIK)

BALB/c mouse model with CT26/HER-2 tumor.¹² This vaccine has completed additional preclinical studies in several animal models to obtain IND and FDA approval for a phase 1 clinical trial.¹⁶ PD1-Vaxx (IMU-201) has completed a 3-dose cohort escalation open label, multicenter, dose escalation phase 1 study (NCT04432207). The vaccine was deemed safe, had no observed DLT's and demonstrated preliminary signs of efficacy. The study will therefore move into Phase 1b with IMU-201 being assessed in combination with atezolizumab.

In the present study, we extend our checkpoint inhibitor strategies and report on the discovery and development of four novel chimeric B-cell peptide epitope vaccines targeting human PD-L1, which aims to induce the body to elicit polyclonal antibodies against PD-1/PD-L1 signaling pathway. Initially, we chose the well-studied murine colon cancer cell line CT26 to preliminary screen the effects of the four predicted PD-L1 epitopes. In order to validate the efficacy of the best identified PD-L1 B-cell epitope vaccine, we used several syngeneic mouse models (i) BALB/c mice challenged with D2F2, D2F2/E2, and 4T1 breast tumor models; and (ii) C57BL/6J mice challenged with MC38, MC38/HER-2 colon carcinoma and B16-F10 melanoma tumor models to further evaluate the effects of the chosen [MVF-PD-L1(130); PDL1-Vaxx] peptide vaccine. We tested the combination of PDL1-Vaxx with the HER-2 vaccine (B-Vaxx) in the D2F2/E2 tumor model.

The results showed the mice immunized with PDL1-Vaxx [MVF-PD-L1(130)] or TT3-PD-L1(130) significantly inhibited tumor growths in 4T1, D2F2, and CT26 in BALB/c mice. The C57BL/6J mice immunized with TT3-PD-L1(130) showed much smaller tumor and longer survival rate versus with PBS group in multiple tumor models of MC38, MC38/HER-2, and B16-F10. Notably, the mice immunized with PDL1-Vaxx plus B-Vaxx significantly enhanced the inhibition of D2F2/E2 tumor growth in BALB/c mice. The mice in this triple immunized group have the highest tumor-free rate and survival rate as compared to the standard anti-mouse PD-L1 mAb (10F.9G2). Finally, we conclude that this newly discovered PD-L1 vaccine may offer a viable and an alternative safe treatment option for cancer patients that are being treated with PD-L1 mAbs and additionally combination treatment for breast/colon HER-2+ cancer patients.

Methods and materials. (Check supplementary for detailed information)

Peptide synthesis

As previously described,¹⁷ Four chimeric PD-L1 B-cell peptides vaccines were made by adding a measles virus fusion peptide (MVF, amino acids 288–302, KLLSLIKGVIVHRLEGVE) or tetanus toxoid (TT3), residue (947–967, FNNFTVSWFL RVPKVSASHL) with a four amino acid residue (GPSL) linker to the PD-L1 peptides.

Animals: Rabbits, C57BL/6J and BALB/c mice

All experiments were performed in accordance with the U.S. Public Health Service Policy on Humane Care and Use of Laboratory Animals and approved by the Ohio State University Institutional Animals Care and Use Committee and detailed in the accepted protocols (2009A0013- R2:2/5/2015-2/5/2018; 2009A0013-R3:1/18/2018-1/18/2021; 2009A0013-R4and11/9/2021-11/9/2024). Animals were purchased from Charles River Laboratories (Wilmington, MA, USA).

Animal immunization

Each dissolved peptide vaccines were emulsified with Montanide ISA720. Immunization followed a 3 times 3 weeks interval strategy. Rabbits received 1 mg/dose intramuscularly (IM) (4 points injection) and mice received 0.1 mg/dose subcutaneously (SC).

Antibody purification

The anti-peptide antibodies from immunized animals were purified by affinity chromatography using protein A/G columns (Pierce brand source of ThermoFisher, Rockford, IL). The concentration was measured by spectrophotometric absorbance at 280 nm.

Cell lines and mouse tumor models

BALB/c mice tumor models: CT26, 4T1, D2F2, and D2F2/E2; C57BL/6J tumor models: MC38, MC38/HER-2, and B16-F10.7 Mouse mammary carcinoma cell line D2F2 and D2F2/E2 cell

4ZQK, PD-L1:Avelumab PD-L1:durvalumab (Protein Data Bank <http://www.rcsb.org> code: 8 M) and PD-L1:atezolizumab (Protein Data Bank <http://www.rcsb.org> code: 5X8L, 5XXY).^{22,23} The PD-L1(130) epitope was synthesized with a Tetanus toxoid (TT3) "promiscuous" T-cell epitope replacing our usual MVF T-cell epitope. There are two reasons for this change: (i) the MVF T-cell epitope is restricted to the H-2d mice strain and cannot be used in the H-2b mice strain precluding its use as a chimeric vaccines to be used in the MC38/C57BL/6J syngeneic model; (ii) the TT3 epitope is a chimeric vaccine construct works in both H-2d and H-2b strains, thus its inclusion in our epitope repertoire. (b): The secondary structure of the four selected peptide sequences was modeled by using PyMOL 3-D modeling software Version 2.4.0 (Schrodinger, New York, NY, USA). The PyMOL User's Manual: <https://pymol.org>. (c): The structure of the PD-1/PD-L1 complex adapted by Zak et al.,^{24,25} key amino acids involved in the interaction between hPD-1 (light blue ribbon model; navy blue amino acid residues) and hPD-L1 (green ribbon model; light green amino acid residues) are illustrated. Amino acids that constitute the central hydrophobic core of the hPD-1/hPD-L1 interface are indicated in yellow. Red letters indicate strands on both PD-1 and PD-L1. (d): Overview of in vivo studies. Scheme of immunization with MVF-PD-L1 B-cell epitopes in New Zealand White rabbits. Rabbits were intramuscularly (i.m.) immunized with 1 mg of each MVF-peptide immunogen dissolved in ddH₂O emulsified (1:1) in Montanide ISA 720 vehicle. The rabbits were boosted with the same doses at 3 weeks interval. Blood was collected via the central auricular artery of each rabbit. The terminal sera were collected at 3Y+3 which is 3 weeks after the last immunization. Scheme of immunization with B-cell epitopes in BALB/c mice (MVF or TT3 linked PD-L1) or C57BL/6J mice (TT3-PD-L1). Mice were subcutaneously immunized with 100 µg of each peptide immunogen dissolved in ddH₂O emulsified (1:1) in Montanide ISA 720 vehicle. The rabbits were boosted with the same doses at 3 weeks interval prior to tumor challenge. Blood was collected as indicated and sera tested for antibody titers by ELISA. 2 weeks after the third immunization (3Y), the mice were engrafted subcutaneously with tumor cells as indicated in each set of experiment. Control mice were treated twice weekly with PBS as negative control or with anti-mouse PD-L1 antibody (clone 10F.9G2) as positive control starting 2 days after tumor challenge, mice were treated during the experimental period. Tumor growths were observed and measured by calipers; (e): Immunogenicity of MVF-PD-1 B-cell epitope vaccines were evaluated by ELISA using peptide-coated plates. The 200 ng/well peptides were used to coat the ELISA plates. Titers are defined as the highest dilution of sera with an absorbance value of 0.2 after subtracting the average of blank wells. (f): Antigenicity of PD-L1 peptide vaccines with human PD-L1 (PDL1, PD1-H5228, HIS tag) coated EISA plates. (g): In vitro CT26 tumor cells growth inhibition assay. 10% or 5% sera from immunized rabbits were used to culture with CT26 tumor cells, the tumor cells proliferation was tested by MTT. Normal cell growth serves as control. One-way ANOVA statistics analysis was performed, ** indicates $p < 0.01$, * indicates $p < 0.05$, ($n > 3$). Only anti-PD-L1(130) showed statistical difference ($p < 0.05$) in tumor growth inhibition with 5% of immunized rabbit sera indicating that this epitope was far superior than the others in inhibiting tumor growth.

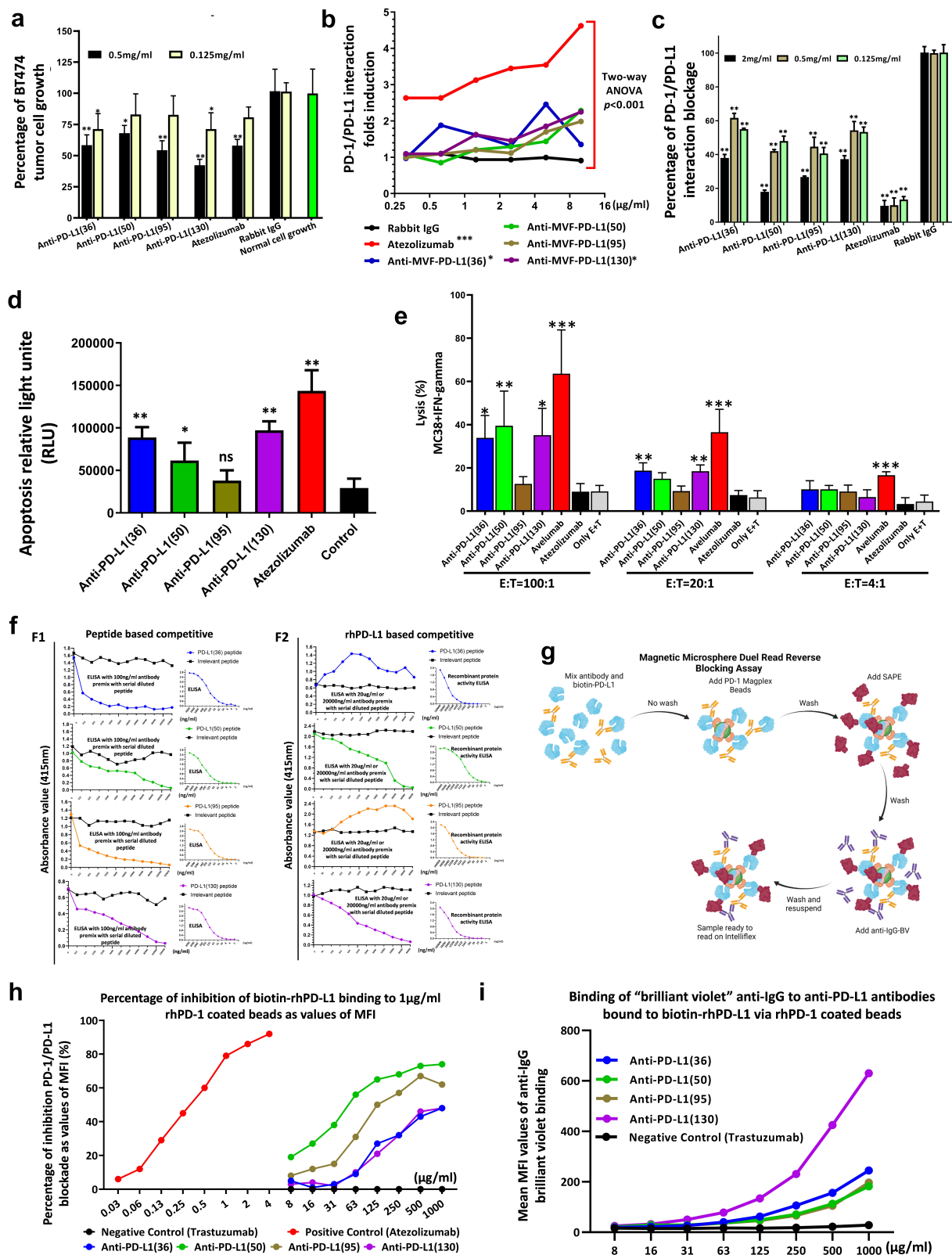


Figure 2. Mechanisms of PD-1/PD-L1 signaling pathway. (a): Antibodies from peptide immunized animals suppress BT474 tumor growth *in vitro* tested by MTT cell proliferation assay, * indicate $p < 0.05$, ** indicate $p < 0.01$ versus with normal cell growth by one-way ANOVA analysis, ($n > 3$); (b): PD-1/PD-L1 interaction luciferase induction assay. The blockade of PD-1/PD-L1 interaction is directly proportional to increased luciferase signal. Two-way ANOVA was used to analyze the whole curves comparison, *** indicates $p < 0.001$, * indicates $p < 0.05$ compared with negative control rabbit IgG; The PD-1 and PD-L1 ligation suppressed TCR activation and attenuated the NFAT responsive luciferase activity. Anti-PD-L1 antibody interrupted the interaction between PD-1 and PD-L1 to release PD-1 signaling and reactive TCR to induce the NFAT luciferase signal. (c): Blockade of the PD-1/PD-L1 interaction by anti-PD-L1 monoclonal antibody atezolizumab and purified anti-MVF-PD-L1 antibodies from immunized rabbit sera. ($n = 3$); (d): The caspase activity was used to evaluate the apoptosis of MC38 cancer cells after treatment as indicated. Each of antibody was used to treat MC38 cells at the concentration of 500 µg/ml. Atezolizumab was used as the positive control. The luminescence of caspase-9 was measured by using a luminometer. One-way ANOVA was performed to analysis each group versus with control. * indicates $p < 0.05$, ** indicate $p < 0.01$ and ns indicate no significance, ($n > 3$). (e): ADCC assay. INF-gamma induced MC38 colon carcinoma cells served as target cells were incubated with different ratio of effector cells (hPBMc) after treatment with 50 µg

line were kindly provided by Professor Wei-Zen Wei (Karmanos Cancer Institute, Wayne State University School of Medicine, Detroit, Michigan, USA).¹⁸ MC38 and MC38/HER-2 tumor cell line was a kind gift from Jeffrey Schlom (National Cancer Institute, Bethesda, Maryland, USA).¹⁹

HEK-293 cell line was transfected with PD-L1 plasmid to overexpression of PD-L1 and was used to perform PD-1/PD-L1 interaction induction assay. BT474 cell line was used to perform cell proliferation assays.

Enzyme-linked immunosorbent assay (ELISA)

Immunogenicity was evaluated by ELISA as laboratory standard protocols.^{12,14} Plates were coated with peptide as antigen overnight. Then blocked with BSA, and then followed by incubating with diluted antibodies and HRP-conjugated secondary antibody. Substrate was added before stopping by 1% SDS. Absorbance was read at 415 nm by Microplate reader.

Modified ELISA-based procedures were used to detect Recombinant protein activity; Antibody isotyping; Blockade of PD-1/PD-L1 interaction; and Competitive ELISA; see supplementary for details.

Cells proliferation assay

The cell proliferation assays were performed according to previous publication^{14,15,17} and Cold Spring Harbor (Long Island, NY, USA) protocol²⁰ by using MTT method.

Cell-based PD-1/PD-L1 interaction blockade assay

The cell-based PD-1/PD-L1 interaction blockade assay was performed by using PD-1: PD-L1 cell-based inhibitor screening assay kit (BPS Bioscience San Diego, CA, USA, catalog #:60,800).

Apoptosis assay

Apoptosis was measured by the readout of caspase activity. Caspase-Glo[®]9 Assay (Promega, Madison, WI, USA) kit was used in the assay following the manufacturer's protocol.

Magnetic microsphere beads-based PD-1/PD-L1 blockade assay

The magnetic microsphere beads-based PD-1/PD-L1 interaction was tested by magnetic beads coupled rhPD-1-HIS interact with rh-PD-L1-biotin pretreated with anti-PD-L1 antibodies or

control mAbs followed by streptavidin-PE incubation, the MFI values were read by xMAP INTELLIFLEX[®] System (Luminex). The decreased signal was detected by anti-PD-L1 antibodies blockade PD-1/PD-L1 interaction by binding with rhPD-L1.

Antibody dependent cellular cytotoxicity (ADCC) assay

ADCC was tested by using aCella-TOX kit (Cell Technology, Fremont, CA, USA). The procedure was according to our previous description^{14,15} and the manufacturer's recommendations.

Statistical analysis

Mice tumor volume were calculated as Formula: Volume (LWW) = (Length × Width × Width)/2. Data statistical analysis was performed by GraphPad Prism 8.1.2 (GraphPad Software, Inc. San Diego, CA, USA) and the indicated statistical analysis. $P < 0.05$ was accepted as statistically significant different.

Results

Prediction and selection of PD-L1 peptides

The selection of candidate B-cell epitopes expressed on the surface of PD-L1 was accomplished by computational aided analysis using six correlates of antigenicity. The details of prediction and selection were described by Kaumaya in previous publications.^{12,21} The best scoring epitopes are then idealized by correlation with known crystal structures of PD-L1.^{22,23} The secondary structure of peptides plays an important role in epitope selection. Four B-cell epitopes of human PD-L1 were chosen and synthesized: they are amino acid 36–53, 50–67, 95–112, and 130–147 (Figure 1a). Figure 1b shows the secondary structure of the 4 PD-L1 epitopes and Figure 1c (left) indicates the structure of the PD-1/PD-L1 complex^{24,25} and (right) depicts the location of PD1-Vaxx and PDL1-Vaxx.

Immunogenicity and antigenicity of four novel human PD-L1 peptide epitopes

All four MVF-PD-L1 epitopes showed high anti-PD-L1 peptide polyclonal antibodies in rabbits (Figure 1d) against the immunizing peptides (Figure 1e) and to the recombinant human PD-L1 protein (PDL1, PD1-H5228, HIS tag) rhPDL1 (Figure 1f). Only anti-PD-L1(36) and anti-PD-L1(130) antibodies significantly inhibited CT26 tumor growth with $p < 0.01$ v.s normal tumor cell growth (Figure 1g).

purified antibodies as indicated. Avelumab was used as positive control and atezolizumab was served as negative control. One-way ANOVA were performed versus with the experiment control only with effector cells and target cells (E + T), *** indicates $p < 0.001$, ** indicates $p < 0.01$ and * indicates $p < 0.05$, ($n \geq 3$); (f) **Competitive ELISA** was used to determine the relative affinities and specificities of the PD-L1 anti-peptide antibodies, left side. Right side is the normal ELISA activity to determine antibody concentration (50%). In the competitive ELISA, the 100 ng/ml antibody were premix with serial diluted peptide as indicated (**panel F1**). PD-L1 human recombinant protein (PDL1, PD1-H5228, HIS tag) based competitive ELISA left side, right side is the normal recombinant protein activity, In the competitive ELISA, 20 $\mu\text{g}/\text{ml}$ antibody premix with serial diluted peptide as indicated (**panel F2**). An irrelevant peptide (left panel of **Figure 2 F1**) was used as control and indicates that no observed inhibition demonstrating the specificity of the PD-L1 peptides (**g-h**): **Mechanisms flow of magnetic microsphere beads-based PD-1/PD-L1 blockade assay**, and PD-1/PD-L1 interaction blockade assay; (l): Binding of anti-IgG brilliant violet to antibodies bound to biotin-PD-L1 via PD-1 beads. Leveraging a dual-detection adaptation of the reverse PD-L1 magnetic microsphere-based blocking assay, binding of biotin-PD-L1 to microsphere-coupled PD-1 was detected concurrently with the binding of biotin-PD-L1 to each anti-PD-L1 antibody. MFI was correlated to the dose of anti-PD-L1 antibody in the reaction. In contrast, in this assay there was no detection of positive control atezolizumab on the microspheres. Similarly, no binding of negative control antibody trastuzumab to the PD-1/PD-L1-microsphere complex was detected.

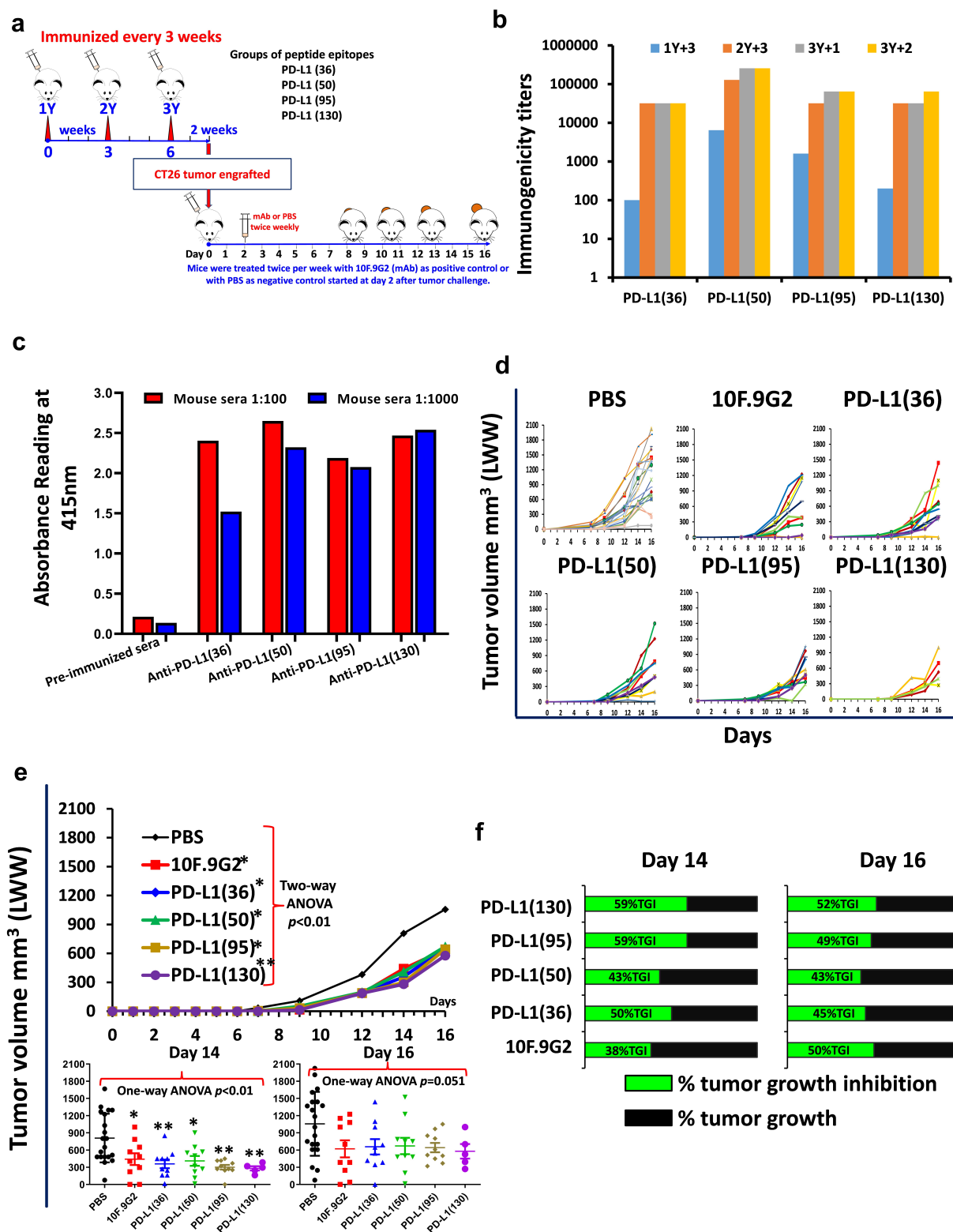


Figure 3. Initial screening of hPD-L1 peptide epitopes in BALB/c mice syngeneic model challenged with CT26 colon carcinoma cell line. (a): Scheme of BALB/c mice vaccination and tumor engraftment. BALB/c mice (PBS, $n = 20$; PD-L1(130), $n = 5$ all other groups $n = 10$) 6–8 weeks old were subcutaneously immunized with MVF-peptide immunogens emulsified in ISA 720 (1:1) with 3 times and three weeks apart. Mice were immunized with 4 MVF-PD-L1 vaccine constructs [PD-L1(36–53), PD-L1(50–67), PD-L1(95–112), PD-L1(130–147)] prior to tumor challenge. Blood was collected as indicated and sera tested for antibody titers by ELISA. 2 weeks after the third immunization (3Y), the mice were engrafted subcutaneously with CT26 tumor cells 10^5 per mouse. Control mice were treated twice weekly with PBS as negative control or with anti-mouse PD-L1 antibody (clone 10F.9G2) as positive control starting 2 days after tumor challenge, mice were treated during the experimental period. Tumor growths were observed and measured by calipers; **(b): Immunogenicity of MVF-PD-L1 peptides in BALB/c mice.** Mice immunized with various peptide constructs. Sera were titered against each individual MVF-PD-L1 peptide immunogen. **(c): Antigenicity.** Mouse sera titered against rhPD-L1. **(d): Individual plots of tumor growths in BALB/c mice** immunized with MVF-PD-L1 vaccine constructs as indicated above, anti-mouse PD-L1 antibody (clone 10F.9G2, PD-L1, B7-H1; Cat#BE0101 BioXCell, Lebanon, NH) as positive control. (PBS $n = 20$; PD-L1(130) $n = 5$; all other groups $n = 10$); **(e): Two-way ANOVA was used to analyze the whole curves of average tumor volume growing**, which shows significant difference between mAb, immunized groups versus PBS group; Plots of tumor volume LWW at day 14 and day 16 for each of group. **(f): Percentage of tumor growth inhibition (%TGI)** was defined as the difference between median tumor volume (MTV) of treatment group with the positive control group and the value was calculated by formula: $\%TGI = 100 \times (\text{MTV control} - \text{MTV test}) / \text{MTV control}$ which were calculated at day 14 and day 16. The %TGI indicate the mice immunized with MVF-PD-L1(36, 50, 95 & 130) showed higher %TGI versus mAb 10F.9G2, especially MVF-PD-L1(95 & 130) had 59% TGI at day 14, only MVF-PD-L1(130) showed 2% higher TGI compared to mAb 10F.9G2 at day 16. “Two-way ANOVA were used for two parameters between two (versus with PBS) or multiple curves comparison; one-way ANOVA followed by Tukey test were used to compare between two groups; $*p < 0.05$, $**p < 0.01$ compared with PBS group”.

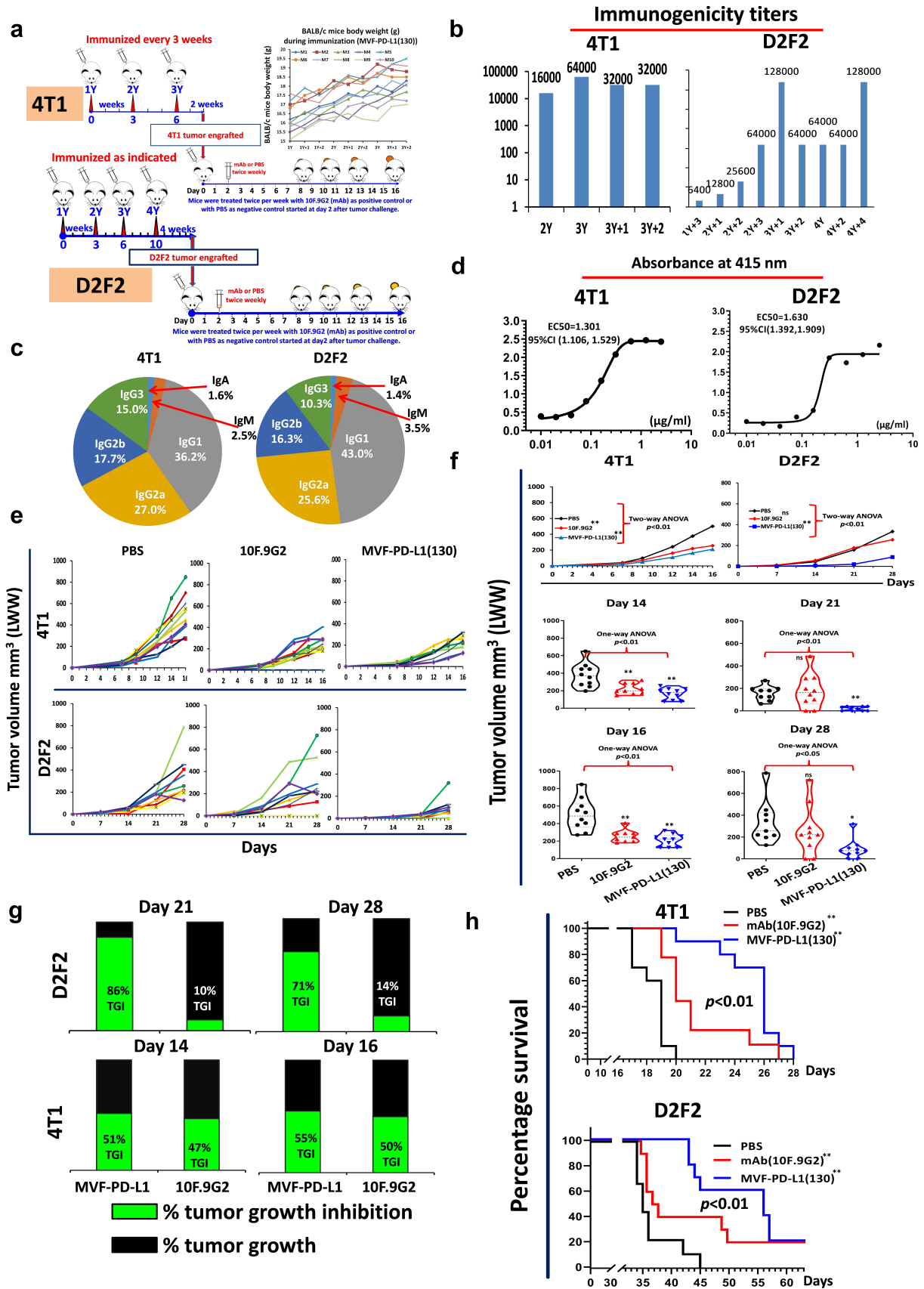


Figure 4. Efficacy of MVF-PD-L1(130) vaccine candidate in BALB/c mice syngeneic model challenged with D2F2 and 4T1 carcinoma cell lines. (a): BALB/c mice (10 mice/gp) 6–8 weeks old were immunized with MVF-PD-L1(130) vaccine emulsified with ISA 720 vehicle with the same scheme as Figure 3a. Four weeks after the last immunization, the mice were challenged with 2×10^5 D2F2 tumor cells. In another set of experiment in a different tumor model, two weeks after the last immunization the mice were subcutaneously injected with 5×10^5 4T1 tumor cells per mouse in each group. The mice in the negative control group were treated with PBS twice weekly whereas mice in the positive control group were *ip* injected with 100 μ l of 2 mg/ml anti-mouse PD-L1 monoclonal antibody (clone 10F.9G2) 2 days after tumor engraftment ($n \geq 9$), mice were treated during the experimental period. (b): Immunogenicity of immunized mice was tested by ELISA. (c): Isotypes in BALB/c mice (sera at the

Antibodies from PD-L1 vaccines immunized animals show enhanced anti-tumor cell proliferation and blockade of PD-1/PD-L1 interactions

Purified antibodies to all 4 PD-L1 epitopes anti-MVF-PD-L1 [(36), (50), (95) & (130)] significantly inhibited BT-474 proliferation at 0.5 mg/ml (Figure 2a). The anti-MVF-PD-L1(130) inhibited cell proliferation at 50% using atezolizumab as control.^{26,27} At the concentration of 0.125 mg/ml, only anti-MVF-[PD-L1 (36) & (130)] significantly decreased cell growth.

As indicated in Figure 2b, anti-MVF-PD-L1 [(130) & (36)] inhibited PD-1/PD-L1 blockade (10 µg/ml) as compared to atezolizumab. On the other hand, Figure 2c shows that all 4 PD-L1 (36, 50, 95 & 130) antibodies block the interaction of PD-L1 with PD-1.

Anti-PD-L1 peptide antibodies induced apoptosis and ADCC of MC-38 cancer cells

MC38 cancer cells were treated with anti-PD-L1 peptide antibodies and caspase-9 were measured by using Caspase-Glo[®]9 kit. All PD-L1 antibodies except 95 induced apoptosis as compared to control (Figure 2d).

The percentage of cell lysis increased for anti-MVF-PD-L1 [(36), (50) & (130)] as indicated in Figure 2e. Avelumab is known to cause ADCC in multiple tumor cells^{28,29} whereas Atezolizumab does not cause ADCC³⁰ (Figure 2e).

Affinity and specificity of PD-L1 antibodies

Competitive ELISA with peptide immunogen coated plates indicated all 4 PD-L1 antibodies showed dose-dependent inhibition with increasing peptide concentration (Figure 2f (F1)). When rhPD-L1 was used as the coating antigen only anti-MVF-PD-L1(50 & 130) antibodies were able to competitively inhibit the binding whereas PD-L1(36 & 95) epitopes were negative. We conclude that all four PD-L1 peptides mimicked the peptide immunogen but only PD-L1 (50 & 130) mimicked the native recombinant protein. Going forward, we are focused on the MVF-PD-L1 (130–147) in several other syngeneic model to further elucidate and enforce its potential as the best vaccine candidate to conduct Phase 1 clinical trials.

Magnetic microsphere beads-based PD-1/PD-L1 blockade assay

We developed a novel magnetic microsphere beads-based PD-1/PD-L1 blockade assay (Figure 2g-2i). Our results

demonstrated that all 4 anti-PD-L1 polyclonal antibodies and atezolizumab inhibited binding of biotin-PD-L1 to PD-1 immobilized on microspheres versus negative control trastuzumab.

Immunogenicity and anti-tumor activity of four MVF-PD-L1 epitopes in a syngeneic BALB/c mice model challenged with CT26 colon tumor cell line

We investigated the effects of the four MVF-PD-L1 peptide vaccine epitopes using validated murine CT26 colon adenocarcinoma BALB/c model (Figure 3a). All four PD-L1 epitopes showed high anti-peptide antibody titers (>100,000) against their respective peptide immunogens (Figure 3b) and exhibited excellent cross activity against rhPD-L1 (Figure 3c). After challenge the tumor growths of individual mice were comparable to the mAb 10F.9G2 group and vaccinated groups (Figure 3d). Two-way ANOVA analysis indicated the peptide immunized mice showed similar tumor control as mAb 10F.9G2 (Figure 3e). The immunized mice showed equivalent tumor growth inhibition compared with the mAb (Figure 3f).

The MVF-PD-L1(130) epitope (PDL1-Vaxx) inhibited tumor growth in syngeneic BALB/c mice challenged with D2F2 and 4T1 tumor cell lines

BALB/c mice were immunized with PDL1-Vaxx and challenged with two carcinoma cell lines (i) 2×10^5 D2F2 tumor cells; (ii) 5×10^5 4T1 tumor cells (Figure 4a). PDL1-Vaxx elicited high titers of anti-PD-L1 polyclonal antibodies (Figure 4b) IgG1 was the predominant isotype, followed by IgG2a and IgG2b. Figure 4c shows high reactivity to rhPD-L1 demonstrating the antigenic potential of the vaccine construct (Figure 4d). Figure 4e shows individual mouse responses. The vaccinated PDL1-Vaxx group and the mAb 10F.9G2 treated group had equivalent and significant reduction in 4T1 tumor growths $p < 0.01$ (Figure 4f). In the D2F2 mice, the PDL1-Vaxx immunized group was more effective in tumor inhibition than the mAb 10F.9G2 group. In the 4T1 model, the PDL1-Vaxx showed slightly higher %TGI versus mAb (Figure 4g). PDL1-Vaxx and mAb 10F.9G2 prolonged survival rate in both models (Figure 4h).

The TT3-PD-L1(130-147) epitope inhibit tumor growth in three different syngeneic BALB/c mice models challenged with CT26 colon carcinoma, D2F2 mammary tumor cells and 4T1 triple-negative mouse breast tumor cell lines

The TT3 epitope was shown to be effective in both H-2D and H-2b mice strains. The efficacy of the TT3-PD-L1(130) epitope in BALB/c mice (Figure 5a) challenged with CT26, D2F2 and

time of tumor challenge were used); The isotypes of PDL1-Vaxx antibodies in the mice sera at the time of tumor challenge were analyzed and the predominant isotype was IgG1 (4T1 group 36.2%) and in the D2F2 model it was 43.0% followed by IgG2a 27.0% in the 4T1 model and 25.6 in the D2F2 model followed by IgG2b 17.7% in the 4T1 model versus 16.3% in the D2F2 model. (d): Recombinant activity of MVF-PD-L1(130) immunized mice sera against human PD-L1 (PDL1, PD1-H5228, HIS tag); (e): Individual plots of D2F2 and 4T1 tumor growths in BALB/c mice immunized with MVF-PD-L1(130) vaccine. Tumor growth in each individual mouse was monitored in both models 4T1 and D2F2 immunized with PDL1-Vaxx or treated with PBS and anti-mouse PD-L1 antibody (clone, 10F.9G2). (f): Plots of D2F2 and 4T1 tumor volume LWW at day 21 and day 28 of D2F2 tumor or at day 14 and day 16 of 4T1 tumor model of each group. Two-way ANOVA was used to analyze the whole curves of tumor growth. (g): Percentage of tumor growth inhibition (%TGI) was defined as the difference between median tumor volume (MTV) of treatment group with the PBS control group and the value was calculated by formula: %TGI = 100*(MTV control-MTV test)/MTV control which were calculated at different days as indicated in the graphs. (h): The log-rank (Mantel-Cox) test was used to compare the survival curves in multiple groups or between two groups (compared with PBS group), * $p < 0.05$, ** $p < 0.01$. Two-way ANOVA were used for two parameters between two (versus with PBS) or multiple curves comparison; one-way ANOVA followed by Tukey test were used to compare between two groups (versus with PBS); ns indicates no significance, * $p < 0.05$, ** $p < 0.01$ compared with PBS group.

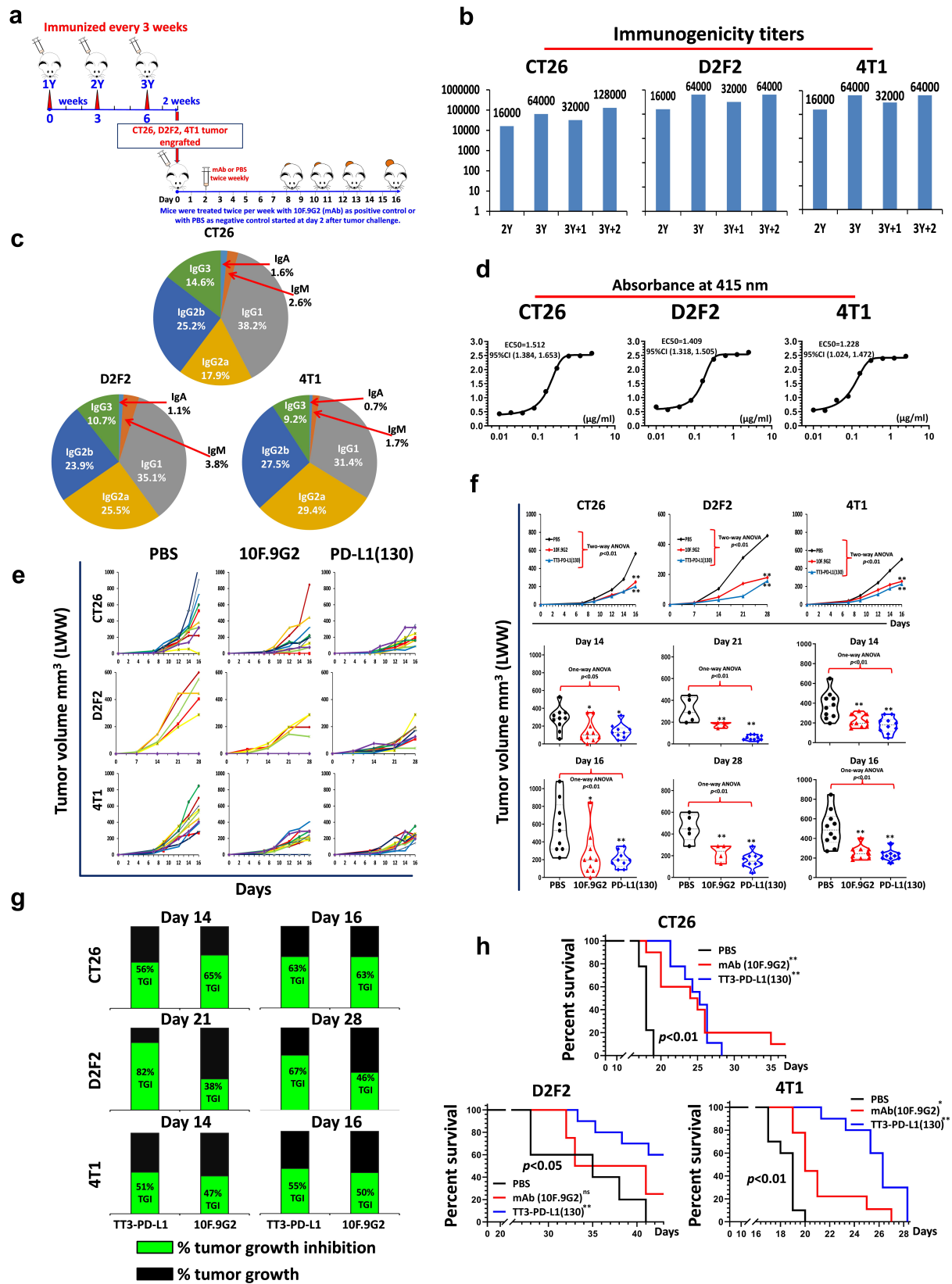


Figure 5. Efficacy of TT3-PD-L1(130) vaccine candidate in BALB/c mice syngeneic model challenged with CT26, D2F2 and 4T1 carcinoma cell lines. (a): Scheme of BALB/c mice vaccination and tumor engraftment. See Figure 1a for more information on TT3 and MVF epitopes. BALB/c mice (10 mice/gp) 6–8 weeks old were immunized with TT3-PD-L1(130) vaccine emulsified with ISA 720 vehicle. Mice were immunized three times and three weeks apart, 2 weeks after the third immunization (3Y), the mice were engrafted with 1×10^5 CT26 tumor cells per mouse, 2×10^5 D2F2 tumor cells per mouse or 5×10^5 4T1 tumor cells per mouse in each group as designed. Control mice were treated twice weekly with PBS as negative control or with anti-mouse PD-L1 antibody (clone 10F.9G2) as positive control group starting on day 2 after tumor challenge, mice were treated during the experimental period. Tumor growths were observed and measured by calipers; Each of the negative control group mice (10 mice/group) were treated with PBS twice per week and positive control group mice were injected with 100 μ l of 2 mg/ml anti-mouse PD-L1 monoclonal antibody (clone 10F.9G2) 2 days after tumor engraftment, twice per week. **(b): Immunogenicity of TT3-PD-L1(130) peptide epitope vaccine in BALB/c mice.** Mice bleeds were collected as indicated after the primary immunization, and ELISA was used to detect antibody titers in sera. For example, the nomenclature 2Y+1 signifies one week post 2nd

4T1 tumor cells. The TT3-PD-L1-130 vaccine elicited high titers of anti-PD-L1 antibody (Figure 5b) against the immunogen. IgG1 was the predominant isotype, followed by IgG2a and IgG2b (Figure 5c). The peptide antibodies showed good cross activity against the native rhPD-L1 protein (Figure 5d).

Mean tumor growth of each group showed that mice immunized with TT3-PD-L1(130) or treated with control mAb 10F.9G2 showed high tumor inhibition compared to the PBS group (Figure 5e). The TT3-PD-L1(130) immunized mice had higher and significant reduction in CT26, D2F2 and 4T1 tumor growths $p < 0.01$ (Figure 5f) as compared to mAb 10F.9G2 treated mice. The TT3-PD-L1 (130) immunized mice showed higher %TGI than mAb 10F.9G2 treated mice (Figure 5g). TT3-PD-L1 (130) and mAb 10F.9G2 prolonged survival rate in CT26, D2F2 and 4T1 cancer models (Figure 5h).

The TT3-PD-L1(130) epitope inhibited tumor growth in syngeneic C57BL/6J mice models challenged with MC38 and MC38/HER-2 colon carcinoma and B16-F10 melanoma tumor cell lines

We tested the efficacy of PD-L1(130) epitope vaccine in a different syngeneic model (C57BL/6J mice) challenged with 3 different carcinoma cell lines: MC38, MC38/HER-2, and B16-F10 tumor cells. C57BL/6J mice were immunized with TT3-PD-L1(130) vaccine (Figure 6a) elicited high titers of anti-PD-L1 antibodies (Figure 6b), and the isotypes were mainly IgG2b followed by IgG1 (Figure 6c). The antibody subtype of IgG2a in C57BL/6J mice was surprisingly different from BALB/c mice. The antibodies showed good cross activity with rhPDL1 (Figure 6d). Upon challenge mice immunized with TT3-PD-L1(130) or treated with mAb 10F.9G2 were more effective in inhibiting tumor growth versus PBS group (Figure 6e) demonstrating equivalent and significant reduction in tumor size for both MC-38 and MC-38/HER-2 $p < 0.01$ (Figure 6f). Interestingly, some mice challenged with B16-F10 tumors did not respond to mAb 10F.9G2 treatment, two mice showed much larger tumor volumes than PBS give group whereas vaccinated mice demonstrated significant tumor growth inhibition. The percentage of tumor growth inhibition for both MC38 and MC38/HER-2 tumor models were equivalent at day 14 and 16 (Figure 6g). The B16-F10 melanoma tumor model, TT3-PD-L1(130) immunized mice showed much greater %TGI than mAb 10F.9G2. This might indicate that TT3-PD-L1(130) showed greater inhibition with the melanoma carcinoma, B16-F10/C57BL/6J mice model.

TT3-PD-L1 (130) and mAb 10F.9G2 demonstrated prolonged survival rate in MC38, MC38/HER-2 cancer models, while only TT3-PD-L1 immunized mice showed statistical longer survival rate and one mouse in mAb 10F.9G2 group survived longer with the latter group showing no statistical difference versus PBS group (Figure 6h).

Immunotherapy with combination of the MVF-PD-L1(130) and B-Vaxx resulted in enhanced tumor inhibition in syngeneic BALB/c-D2F2/E2 mammary tumor model

Combination therapy of PDL1-Vaxx with B-Vaxx (an herceptin-like and perjeta-like HER-2 vaccine) developed in our labs was tested in the D2F2/E2 BALB/c model. In the present study, we tested (i) whether PD1-Vaxx combined with B-Vaxx would have the same efficacy in the D2F2/E2 tumor model versus the initial CT26/HER-2 BALB/c model; (ii) Additionally, we tested efficacy of combining B-Vaxx with PD1-Vaxx versus PDL1-Vaxx.

The immunized mice were injected with B-Vaxx, and triple vaccine combination of MVF-PD-1(92) + B-Vaxx and MVF-PD-L1(130) + B-Vaxx (Figure 7a). Robust B-Vaxx, PD1-Vaxx and PDL1-Vaxx antibody responses were obtained in all the immunized groups as determined by ELISA (Figure 7b) indicating that all epitopes were highly immunogenic. The antibodies in the mice sera were analyzed, and the isotypes were IgG1 followed by IgG2a and IgG2b for PD-1, PD-L1 and HER-2 (Figure 7c). The activity against recombinant human HER-2 protein indicates the antibody in the triple immunized mice sera have higher EC50 versus combo treatment mice. Furthermore, the reaction with rhPD-L1 shows the mice without tumor or CR mice (tumor-free mice) or mice with very small tumors 8 weeks after challenge have significant higher EC50 than the mice without complete response with large tumor burden (Figure 7d). Tumor growth of individual mouse in each group showed that the mice immunized with B-Vaxx or PD1-Vaxx plus B-Vaxx or PDL1-Vaxx plus B-Vaxx had no tumors at day 21 and day 28 (Figure 7e). Few mice had small tumors in combo HER-2 and PD-1 triple groups. The B-Vaxx alone or combined with PD1-Vaxx or with PDL1-Vaxx showed dramatically significant tumor inhibition than the gold standard anti-mouse PD-1 mAb 29F.1A12 and anti-mouse PD-L1 mAb 10F.9G2 (Figure 7f). Almost all the immunized mice were completely protected at day 28 except one mouse in combo HER-2 group had a small tumor. The percentage of tumor growth inhibition was lower for mAb 10F.9G2 than for

injection; 3Y+2 signifies 2 weeks post 3rd injection etc; (c): Isotypes in BALB/c mice (3Y+2) after immunization with TT3-PD-L1(130) and ISA 720. The class of antibodies in mice sera elicited by vaccination with TT3-PD-L1(130) were analyzed by using mouse specific isotyping kit. (d) Antigenicity of TT3-PD-L1(130) peptide epitope vaccine in BALB/c mice using human recombinant protein PD-L1 (PDL1, PD1-H5228, HIS tag); (e): Individual plots of tumor growths in BALB/c mice immunized with TT3-PD-L1 vaccine, PBS as negative control and anti-mouse PD-L1 antibody (clone 10F.9G2) as positive control. (f): Plots of tumor volume LWWat day 14 and day 16 for CT26 and 4T1 models or day 21 and day 28 for D2F2 tumor model of each group. Two-way ANOVA was used to analyze the whole curves of tumor growth, which shows significant difference with $p < 0.01$, one-way ANOVA was used to analyze the multiple groups comparison; (g): Percentage of tumor growth inhibition (%TGI) was defined as the difference between median tumor volume (MTV) of treatment group with the PBS control group and the value was calculated by formula: %TGI = $100 * (MTV \text{ control} - MTV \text{ test}) / MTV \text{ control}$ which were calculated at different days as indicated in the graphs. (h): The Log-rank (Mantel-Cox) test was used to compare the survival curves in multiple groups or between two groups (compared with PBS group), * $p < 0.05$, ** $p < 0.01$. Two-way ANOVA were used for two parameters between two (versus with PBS) or multiple curves comparison, one-way ANOVA followed by Tukey test were used to compare between two groups (versus with PBS group); ns indicates no significance, * indicates $p < 0.05$, ** indicate $p < 0.01$.

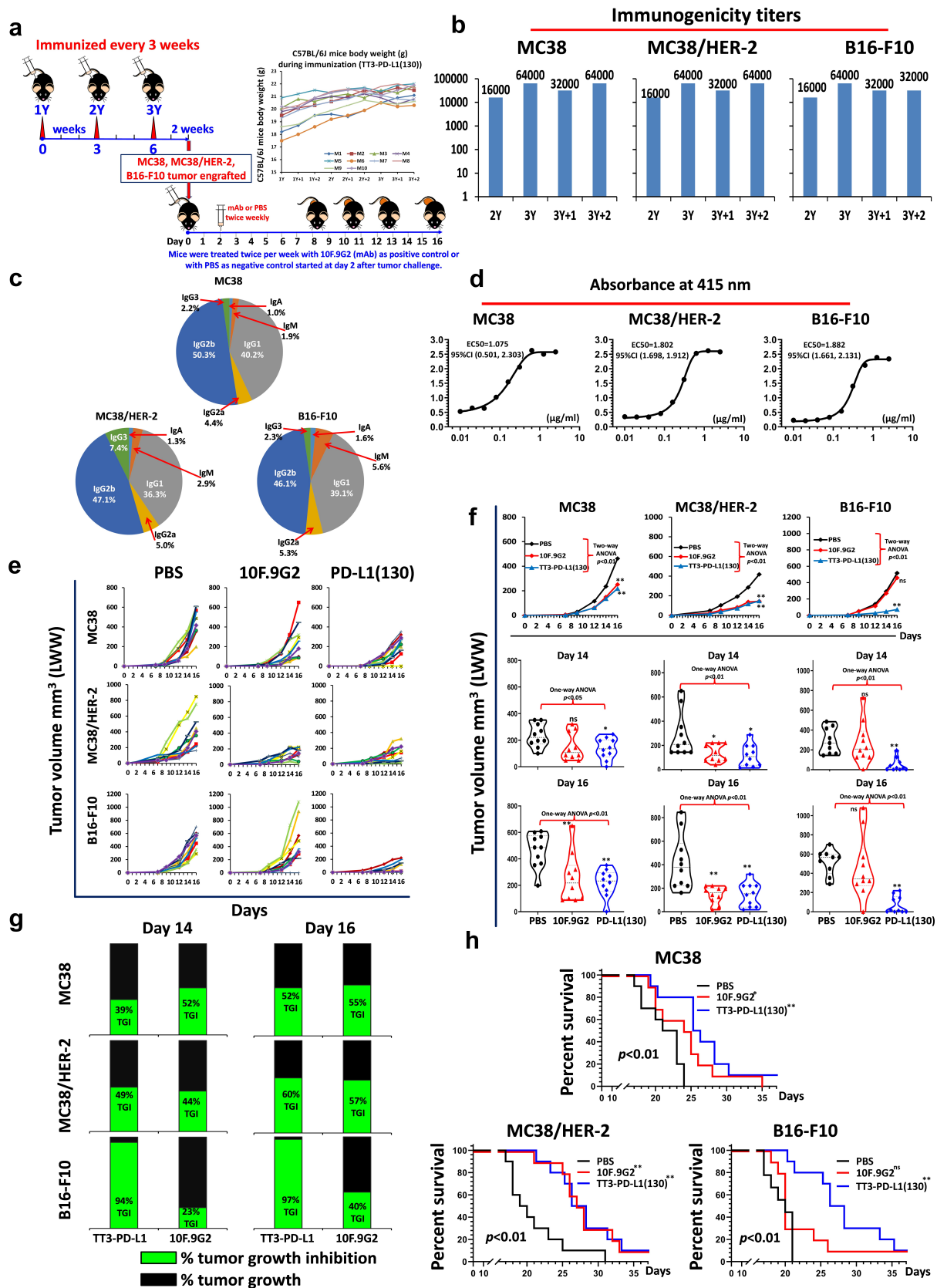


Figure 6. Efficacy of TT3-PD-L1(130) vaccine candidate in C57BL/6J black mice syngeneic model challenged with MC38 wild type, MC38/HER-2 and B16-F10 carcinoma cell lines. (a): Scheme of C57BL/6J mice vaccination and tumor engraftment. The mice (10 mice/gp) 6–8 weeks old were immunized with TT3-PD-L1(130) vaccine emulsified with ISA 720 vehicle. Mice were immunized three times and three weeks apart, 2 weeks after the third immunization (3Y), the mice were engrafted with 1×10^5 MC38 wild-type tumor cells per mouse, 1×10^5 MC38/HER-2 tumor cells per mouse or 1×10^5 B16-F10 tumor cells per mouse in each group as designed. Control mice were treated twice weekly with PBS as negative control or with anti-mouse PD-L1 antibody (clone 10F.9G2) as positive control group starting on day 2 after tumor challenge, mice were treated during the experimental period. Tumor growths were observed and measured by calipers; (b): Immunogenicity of TT3-PD-L1(130) peptide epitope vaccine in C57BL/6J mice. Mice bleeds were collected as indicated after the primary immunization, and ELISA was used to detect antibody titers in sera. (c): Isotypes in C57BL/6J mice (3Y+2) after immunization with TT3-PD-L1(130) and ISA 720; (d): Antigenicity of TT3-PD-L1(130) in mice using human recombinant protein PD-L1

mAb 29F.1A12. While all the immunized mice in the D2F2/E2 mammary tumor model had over 98% TGI demonstrating the effectiveness of combination immunotherapy (Figure 7g). The survival rate in Figure 7h indicates combo and triple vaccinated groups were more effective than mAb or control groups. All tumor-free mice were boosted at day 70, and the mice were re-challenged on day 91 after primary challenge (Figure 7i). Figure 7j shows the immunogenicity of the re-challenged mice. Tumor growth within the combination treatments with triple vaccines showed significantly less tumor burden and prolonged survival (Figure 7k, l). The high survival rates in the triple treatment groups suggest that inhibiting multiple cancer signaling targets with combination peptide-based vaccines may demonstrate enhanced synergistic tumor inhibition compared to single vaccine treatments.

Discussion

Immune checkpoint blockade with antibodies is presently the favored immunotherapeutic strategy in the clinic with several FDA approved drugs. PD-L1 is deemed an ideal target to develop a vaccine in the checkpoints landscape because of its minimal expression in normal tissues with great overexpression on tumor cells. The development of more efficacious, increased specificity and safer medicine is warranted given the present landscape in the field. Engineered peptide vaccines eliciting a durable polyclonal antibody response with potent anti-tumor effects that blocks PD-1/PD-L1 pathway could be a favored approach with substantial advantages over existing therapies.^{12,31–33}

Small molecule checkpoint inhibitors have emerged as potential alternatives to mAbs treatment^{34–36} potentially overcoming the mAb issues, but they also suffers from numerous shortcomings. An orally bioavailable small molecule checkpoint inhibitor CA-170 have been developed as a dual inhibitor of PD-L1 and VISTA. CA170 exhibits desirable pharmacological and safety features such as oral dosing has now progressed to the clinic (Phase 1 completed; ClinicalTrials.gov Identifier: NCT02812875).³⁷

There have been several attempts to develop potential PD-L1 vaccines that block the interaction with PD-1 because targeting PD-L1 offers certain beneficial properties.

Accumulating evidence of preclinical studies and clinical trials have demonstrated that the PD-1/PD-L1 axis is critical for tumor to avoid the immune system to allow growth and blocking the PD-1/PD-L1 interaction showed effective anti-tumor outcomes.^{38,39}

Yao and Gao group used the murine PD-L1 extracellular domain (ECD) (19–239) and human PD-L1 ECD (19–238) generated two nitrated T – cell epitope vaccines, mPDL1-NitraTh and hPD-L1-NitraTh.⁴⁰ The full PDL1 extracellular

domain vaccine “PD-L1-NitraTh” increased the infiltration of tumor lymphocytes and decreased the proportion of Treg cells in tumor tissues, which exhibited potent antitumor activity. Li’s group developed a PD-L1-based cancer vaccine, DPDL1E, by using mouse PD-L1 sequence. In a mouse melanoma model, DPDL1E elicited robust immune responses biased towards the Th1 type and inhibited tumor growth in both B16-F10-C57BL/6J and CT26-BALB/c mice models.⁴¹

In the current study, we are extending our checkpoint inhibition approach by developing a PD-L1 vaccine. We engineered 4 PD-L1 peptide epitopes (Figure 1a) and demonstrated high immunogenicity and antigenicity (Figure 1e, f, g). We assessed the efficacy of PD-L1 epitopes *in vivo* in a syngeneic BALB/c/CT26 model which demonstrated enhanced tumor inhibition (Figure 2). We also determined the properties of each of the PD-L1 epitopes through a series of *in vitro* assays (ADCC, apoptosis, inhibition of proliferation and PD-1/PD-L1 blockade) (Figure 3) that allowed us to select MVF-PD-L1(130) as the most efficacious vaccine. In order to further establish that the MVF-PD-L1(130) termed (PDL1-Vaxx) as the vaccine of choice, we conducted a series of syngeneic BALB/c mouse studies utilizing two different cell lines D2F2 and 4T1 (Figure 4). When mice were challenged with those two carcinoma cell lines, the PDL1-Vaxx vaccine exhibited enhanced tumor inhibitory properties when compared to the anti-PDL1 mouse mAb (10F.9G2).

In order to extend the validity of our chosen PD-L1 (130–147) epitope, we chose a different C57BL/6J syngeneic mouse model and tested the efficacy in 3 challenge models utilizing MC38, MC38/HER-2 and B16-F10 carcinoma cells. Next, we also redesigned the PDL1-Vaxx (MVF-PD-L1-130) to incorporate a different “promiscuous” T-cell epitope (Tetanus toxoid, TT3) because the MVF “promiscuous” T-cell epitope is not immunogenic in C57BL/6J. Given that the TT3 epitope is equally effective⁴² in conferring immunogenicity in both BALB/c and C57BL/6J mice, we initially tested the TT3-PD-L1(130) epitope in the BALB/c model challenged with CT26, D2F2 and 4T1. The vaccine was highly immunogenic/antigenic (Figure 5b, 5d) and was equally effective in inhibiting tumor growth as compared to anti-PDL1 mouse mAb. In the C57BL/6J mice model and in the MC38 and MC38/HER-2 tumor challenge model, the TT3-PD-L1(130) was equally effective as the anti-PDL1 mouse mAb, however in the B16-F10 model the TT3-PD-L1(130) showed outstanding inhibitory properties as compared to the control PD-L1 mAb (Figure 6). “As we can see, the immunized mice show comparable or better tumor inhibition than mAb. While, mAb (avelumab, atezolizumab) is more efficacious in the

(PDL1, PD1-H5228, HIS tag); (e): Individual plots of tumor growths in C57BL/6J mice immunized with TT3-PD-L1(130) vaccine, PBS as negative control and anti-mouse PD-L1 antibody (clone 10F.9G2) as positive control. (f): Plots of tumor volume LWW at day 14 and day 16 for MC38 wild type, MC38/HER-2 and B16-F10 models of each group. Two-way ANOVA was used to analyze the whole curves of tumor growth, which shows significant difference with $p < 0.01$, one-way ANOVA was used to analyze the multiple groups comparison; (g): Percentage of tumor growth inhibition (%TGI) was defined as the difference between median tumor volume (MTV) of treatment group with the PBS control group and the value was calculated by formula: %TGI = $100 \times (\text{MTV control} - \text{MTV treatment}) / \text{MTV control}$ which were calculated at different days as indicated in the graphs. (h): The Log-rank (Mantel-Cox) test was used to compare the survival curves in multiple groups or between two groups (compared with PBS group), * $p < 0.05$, ** $p < 0.01$. Two-way ANOVA were used for two parameters between two (versus with PBS) or multiple curves comparison; one-way ANOVA followed by Tukey test were used to compare between two groups (versus with PBS group); ns indicates no significance, * indicates $p < 0.05$, ** indicate $p < 0.01$.

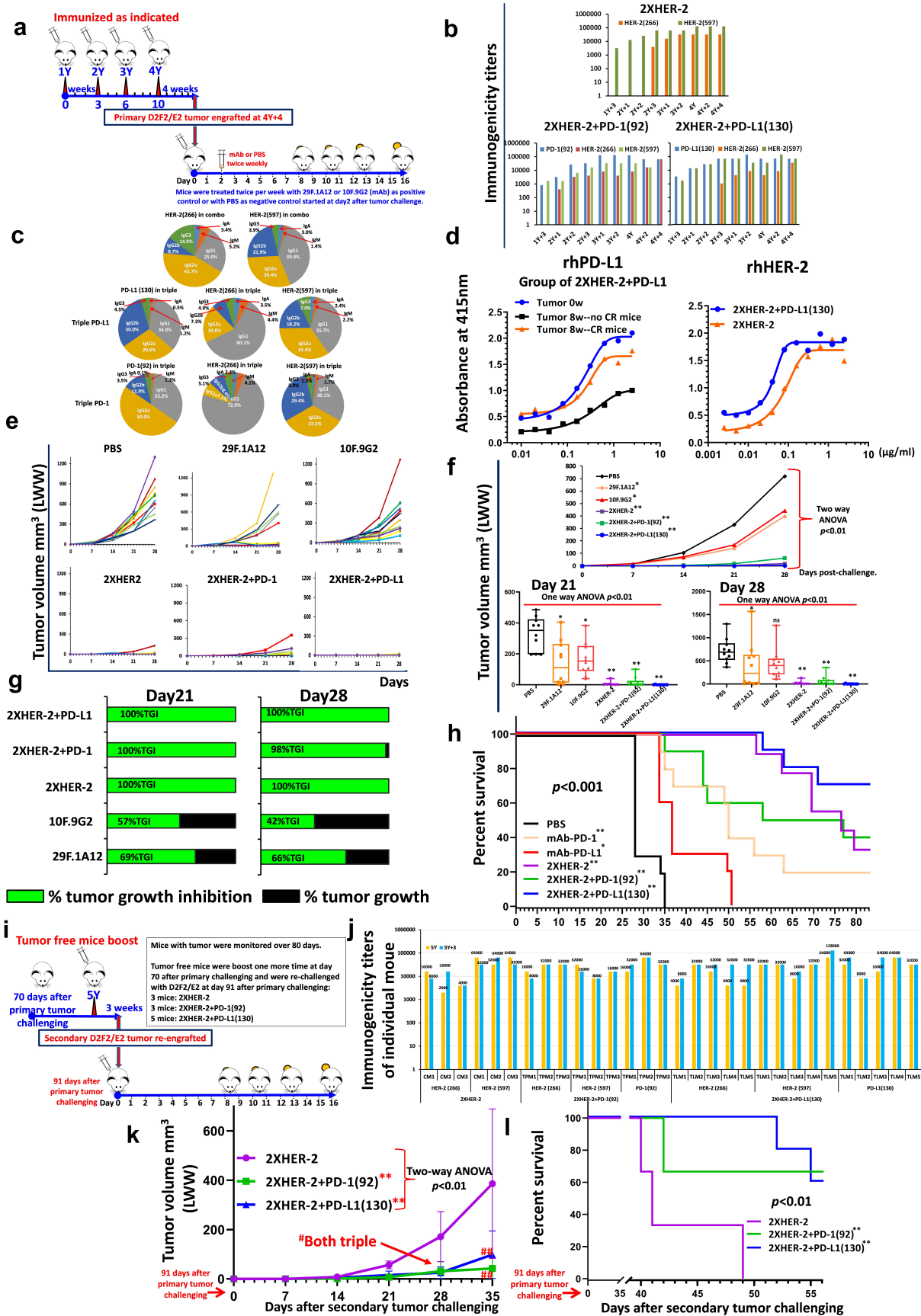


Figure 7. Efficacy of combination treatment of MVF-PD-L1(130) vaccine and combo HER-2 vaccines in syngeneic BALB/c mice model challenged with D2F2/E2 mammary tumor cells. (a): Scheme of BALB/c mice vaccination and tumor engraftment. BALB/c mice (10 mice/gp) 6–8 weeks old were immunized with **combo** HER-2: [MVF-HER-2(266) + MVF-HER-2(597)], **triple**: [MVF-PD-1(92) + combo HER-2] and **triple**: [MVF-PD-L1(130) + combo HER-2] vaccine emulsified with ISA 720 vehicle. Mice were immunized at least three times, and three weeks apart, and the mice were engrafted with 2×10^5 D2F2/E2 tumor cells per mouse in each group as designed. Control mice were treated twice weekly with PBS as negative control or with anti-mouse PD-1 antibody (clone 29F.1A12) or anti-mouse PD-L1 antibody (clone 10F.9G2) as

in vitro analysis than vaccine induced poly-clonal antibodies which are broadly multifunctional as compared to mono-clonal antibodies. The in vivo study is a more complex system within the microenvironment. That might lead to precise therapeutic strategies due to the response from each individual might be different.”

Notably, in the D2F2/E2 BALB/c syngeneic mammary tumor model, combination HER-2 plus PD-L1 immunized group showed significant tumor growth inhibition and dramatically prolonged mice survival rate over all other groups. Especially, 50% (5 out of 10) mice in the combination HER-2 plus PD-L1 immunized group showed tumor free after primary tumor challenging. After one more boost (5Y) and the tumor-free mice were re-challenged with D2F2/E2. PD-L1 plus B-Vaxx immunized mice showed lower tumor burden and longer survival (Figure 7). These data suggest B-Vaxx and PDL1-Vaxx combination showed the greatest inhibition of tumor growth and prevention of recurrence.

Targeting both HER-2 and PD-1/PD-L1 signaling pathways are of great clinical significance exemplified by the accelerated approval of the combination of pembrolizumab with trastuzumab for HER-2+ gastric cancer in 2021. We also have demonstrated that a combination treatment of PD1-Vaxx with B-Vaxx had synergistic inhibition of tumor growth in BALB/c/CT26/HER-2 model.¹² This exemplifies the potential clinical benefit of combining cancer vaccines with checkpoint inhibition. In this present work, we tested the synergistic combination of **PDL1-Vaxx and PD1-Vaxx** vaccination with **B-Vaxx** in the D2F2/E2 challenge model. The results show that combination therapy of B-Vaxx with either PD-L1 or PD-1 had synergistic tumor inhibitory properties than either PDL1 or PD1 mAb positive controls. Recently, a humanized bispecific IgG1 subclass antibody targeting HER-2 and PD-L1 inhibited tumor growth with superior efficacy and enhanced ADCC.⁴³ Similarly, another group developed

a bispecific antibody simultaneously targeting PD1 and HER-2 that inhibited tumor growth by combination of PD1/PDL1 blockade and HER-2 inhibition.⁴⁴ This supports the combination cancer therapy with B-cell vaccines combined and/or with monoclonal antibodies, as the future of clinical cancer treatment.

Conclusion

We can conclude a potential PD-L1 vaccine candidate has been identified that could be used in combination immunotherapy clinical trials. The antibodies generated from PD-L1 vaccination can induce apoptosis and ADCC. Taken together, with effectively blocking the PD-1/PD-L1 pathway, the vaccine is efficacious in inhibiting tumor growth in multiple tumor syngeneic models. The combination of immune checkpoints targeted vaccines or with other traditional cancer therapeutic treatment should be the priority consideration in the clinical oncology landscape. B-cell peptide-based vaccines targeting HER-2 and PD-1 have successfully completed Phase I and II clinical trials B-cell vaccines being shown to be well-tolerated and with promising response data. We expect our latest peptide-based PDL1-Vaxx will join our B-cell vaccine family to give the benefit to clinical patients.

Highlights

- PDL1-Vaxx is a novel checkpoint inhibitor B-cell epitope peptide vaccine incorporating a “promiscuous” T-cell epitope
- PDL1-Vaxx elicited antibodies can induce apoptosis, ADCC and effectively block the PD-1/PD-L1 pathway
- PDL1-Vaxx demonstrated enhanced tumor inhibition, prolonged anti-tumor responses in multiple syngeneic cancer models
- Combination of PDL1-Vaxx with HER-2 vaccine (B-Vaxx) results in synergistic tumor inhibition in D2F2/E2-BALB/c cancer model

positive control groups starting on day 2 after tumor challenge, mice were treated during the experimental period. Tumor growths were observed and measured by calipers; D2F2/E2 is generated from a BALB/c mouse background mammary carcinoma D2F2 cell line that can express human HER-2 on the cell surface.¹⁸ This cell line was a kind gift from Wei-Zen Wei (School of Medicine, Wayne State University, Detroit, MI). **(b): Immunogenicity of combo and triple vaccinations in BALB/c mice.** Mice bleeds were collected as indicated after the primary immunization, and ELISA was used to detect antibody titers in sera. **(c): Isotypes in BALB/c mice** (sera at the time of tumor challenge were used) after immunization; **(d): Antigenicity of combo and triple vaccinations in BALB/c mice** using human recombinant protein PD-L1 (PDL1, PD1-H5228, HIS tag) or human recombinant HER-2 (HE2-5225 HIS tag) activity of mice sera at the time of tumor challenge; **(e): Individual plots of tumor growths in BALB/c mice** immunized with combo or triple vaccines, PBS as negative control and anti-mouse PD-1 antibody (clone 29F.1A12) or anti-mouse PD-L1 antibody (clone 10F.9G2) as positive controls. **(f): Plots of tumor volume LWW** at day 21 and day 28 of D2F2/E2 tumor model of each group. Two-way ANOVA was used to analyze the whole curves of tumor growth, which shows significant difference with $p < 0.01$, one-way ANOVA was used to analyze the multiple groups comparison; **(g): Percentage of tumor growth inhibition (%TGI)** was defined as the difference between median tumor volume (MTV) of treatment group with the PBS control group and the value was calculated by formula: %TGI = 100*(MTV control-MTV test)/MTV control which were calculated at different days as indicated in the graphs. **(h): The Log-rank (Mantel-Cox) test** was used to compare the survival curves in multiple groups $p < 0.001$. **(i): Scheme of tumor free immunized BALB/c mice re-engraftment.** 3 mice in combo 2xHER-2 group (named CM1, CM2, and CM3), 3 mice in triple 2xHER-2+ PD-1(92) group (named TPM1, TMP2, and TMP3), 5 mice in triple 2xHER-2+ PD-L1(130) group (named TLM1, TLM2, TLM3, TLM4, and TLM5) were boosted with the same vaccines at 10-week (70 days) after the primary tumor challenging (named as 5Y, which is 4Y+14), 3 weeks later (5Y+3), each individual mouse bleed were collected and each mouse was challenged (which was 91 days after the primary tumor challenging) with 5×10^5 D2F2/E2 tumor cells. The tumor growth was monitored. **(j): Immunogenicity of each mouse** at 5Y and 5Y+3 tested by ELISA. **(k): Each group of tumor volume (mm³, LWW) showed as line curves, ($n \geq 3$), values of mean \pm SD. Two-way ANOVA followed Dunnett’s multiple comparisons test was performed to analyze the data. **indicates 2xHER-2+ PD-1(92), and 2xHER-2+ PD-L1(130) group showed significantly slower ($p < 0.01$) tumor growth compared with 2xHER-2 group. Both at day28 and day35, 2xHER-2+ PD-1(92), and 2xHER-2+ PD-L1(130) group mice with significantly smaller tumor versus 2xHER-2 group, # $p < 0.05$, ## $p < 0.01$, respectively. **(l): The Log-rank (Mantel-Cox) test** was used to compare the survival curves, $p < 0.01$. Two-way ANOVA were used for two parameters between two groups (versus with PBS group) or multiple curves comparison; one-way ANOVA followed by Tukey test were used to compare between two groups (versus with PBS group); the Log-rank (Mantel-Cox) test was used to compare the survival curves in multiple groups or between two groups (for between groups, in (H) versus with PBS group, in (I) versus with 2xHER-2 group). ns indicates no significance, * indicates $p < 0.05$, ** indicates $p < 0.01$.**

List of abbreviations

Ab:	Antibody;
ABTS:	2, 2'-aminobis (3-ethylbenzthiazole- 6-sulfonic acid)
ADCC:	Antibody dependent cellular cytotoxicity;
ANOVA:	Analysis of variance;
ATCC:	The American Type Culture Collection;
BSA:	Bovine serum albumin;
B16-F10:	C57BL/6J mouse melanoma cell line;
B-Vaxx:	HER-2 Peptide B cell vaccine combination MVF-HER-2(266) and MVF-HER-2(597);
CTLA-4:	Cytotoxic T lymphocyte antigen 4;
CT26:	BALB/c mouse colon tumor cell line;
CCIC:	Campus Chemical Instrumentation Center;
D2F2:	BALB/c mouse mammary tumor cell line;
D2F2/E2:	BALB/c mouse mammary tumor cell line expresses human HER-2
EDT:	Ethane-1,2-dithiol;
ELISA:	Enzyme-linked immunosorbent assay;
FDA:	U.S. Food and Drug Administration
GPLS:	Four amino acid residues, Glycine-Proline-Serine-Leucine;
INF-gamma:	Interferon gamma;
LWW	Tumor volume(LWW) = (Length X Width X Width)/2
MALDI:	Matrix-Assisted Laser Desorption Ionization;
MVF:	Measles virus fusion peptide residue;
MTV:	Median tumor volume;
MC38:	C57BL/6J mouse colon carcinoma cell line;
MC38/HER-2:	C57BL/6J mouse colon carcinoma cell line expresses human HER-2;
NSCLC:	Non-small-cell lung cancer;
PBS:	Phosphate-buffered saline;
PD-1:	Programmed cell death protein 1;
PD1-Vaxx:	PD-1 peptide vaccine MVF-PD-1(92-110);
PD-L1:	Programmed cell death protein 1 ligand;
PDL1-Vaxx:	PD-L1 peptide vaccine MVF-PD-L1(130-147);
RP-HPLC:	Reversed phase high performance liquid chromatography;
SDS:	Sodium dodecyl sulfate;
TT3:	Tetanus toxoid residue;
TFA:	Trifluoroacetic acid;
ULAR:	University Laboratory Animal Resources;
4T1:	BALB/c mouse triple-negative breast cancer cell line;
%TGI:	Percentage of tumor growth inhibition;

Acknowledgments

The authors thank Dr. Jeffrey Schlom (National Cancer Institute, Bethesda, Maryland USA) who provided us with MC38 and MC38/HER-2 tumor cell lines and Professor Wei-Zen Wei (School of Medicine, Way State University, Detroit, MI) who provided us with D2F2 and D2F2/E2 cell lines.

Disclosure statement

Pravin T.P. Kaumaya is consultant to Imugene, Ltd. Nicholas Ede is CTO at Imugene. All the other authors declare no competing interests. Heather Darby is now at Assurance laboratories, Birmingham, AL. (hdarby@assurancelabs.com).

Author's contributions

Concept and Design: PTPK; development of methodology: LG, JO, PTPK; acquisition of data: LG, JO; study supervision: PTPK; analysis and

interpretation of data: PTPK, LG, JO, NJE; writing, review of manuscript: LG, JO, NJE, PTPK

Data availability statement

Most data relevant to this study are included in the article or uploaded as supplemental files. Other data information's available on reasonable request from corresponding author.

Ethics approval and consent to participate

All animal experiments were in compliance with the regulations and guidelines of the Ohio State University and were conducted according to the IACUC guidelines and accepted in the approved protocols (2009A0013- R2:2/5/2015-2/5/2018; 2009A0013-R3:1/18/2018-1/18/2021; 2009A0013-R4and11/9/2021-11/9/2024). Animals were purchased from Charles River Laboratories (Wilmington, MA, USA).

Consent for publication

All authors have reviewed and approved the final version of the manuscript.

Funding

This work was supported by the NIH [R21 CA13508]; NIH [R01 CA84356]; Imugene Ltd [OSU 900600] to Pravin T. P. Kaumaya; NIH; IMUGENE ltd [GR110567; GR124326, R21 CA13508, R01 CA84356, IMUGENE 900600.

ORCID

Pravin T.P Kaumaya  <http://orcid.org/0000-0002-8647-3911>

References

- Ott PA, Hodi FS, Robert C. CTLA-4 and PD-1/PD-L1 blockade: new immunotherapeutic modalities with durable clinical benefit in melanoma patients. *Clin Cancer Res.* 2013;19(19):5300–5309. doi:10.1158/1078-0432.CCR-13-0143.
- Robert C, Thomas L, Bondarenko I, O'Day S, Weber J, Garbe C, Lebbe C, Baurain J-F, Testori A, Grob -J-J, et al. Ipilimumab plus dacarbazine for previously untreated metastatic melanoma. *N Engl J Med.* 2011;364(26):2517–2526. doi:10.1056/NEJMoa1104621.
- Topalian SL, Hodi FS, Brahmer JR, Gettinger SN, Smith DC, McDermott DF, Powderly JD, Carvajal RD, Sosman JA, Atkins MB, et al. Safety, activity, and immune correlates of anti-PD-1 antibody in cancer. *N Engl J Med.* 2012;366(26):2443–2454. doi:10.1056/NEJMoa1200690.
- Brahmer JR, Tykodi SS, Chow LQ. Safety and activity of anti-PD-L1 antibody in patients with advanced cancer. *N Engl J Med.* 2012;366(26):2455–2465. doi:10.1056/NEJMoa1200694.
- Hodi FS, O'Day SJ, McDermott DF, Weber RW, Sosman JA, Haanen JB, Gonzalez R, Robert C, Schadendorf D, Hassel JC, et al. Improved survival with ipilimumab in patients with metastatic melanoma. *N Engl J Med.* 2010;363(8):711–723. doi:10.1056/NEJMoa1003466.
- Agata Y, Kawasaki A, Nishimura H. Expression of the PD-1 antigen on the surface of stimulated mouse T and B lymphocytes. *Int Immunol.* 1996;8(5):765–772. doi:10.1093/intimm/8.5.765.
- Vibhakar R, Juan G, Traganos F. Activation-induced expression of human programmed death-1 gene in T-lymphocytes. *Exp Cell Res.* 1997;232(1):25–28. doi:10.1006/excr.1997.3493.

8. Iwai Y, Ishida M, Tanaka Y, Okazaki T, Honjo T, Minato N. Involvement of PD-L1 on tumor cells in the escape from host immune system and tumor immunotherapy by PD-L1 blockade. *Proc Natl Acad Sci U S A*. 2002;99(19):12293–12297. doi:10.1073/pnas.192461099.
9. Sharpe AH, Pauken KE. The diverse functions of the PD1 inhibitory pathway. *Nat Rev Immunol*. 2018;18(3):153–167. doi:10.1038/nri.2017.108.
10. Freeman GJ, Long AJ, Iwai Y, Bourque K, Chernova T, Nishimura H, Fitz LJ, Malenkovich N, Okazaki T, Byrne MC, et al. Engagement of the PD-1 immunoinhibitory receptor by a novel B7 family member leads to negative regulation of lymphocyte activation. *J Exp Med*. 2000;192(7):1027–1034. doi:10.1084/jem.192.7.1027.
11. Shukuya T, Carbone DP. Predictive markers for the efficacy of Anti-PD-1/PD-L1 Antibodies in lung cancer. *J Thorac Oncol*. 2016;11(7):976–988. doi:10.1016/j.jtho.2016.02.015.
12. Kaumaya PTP, Guo L, Overholser J, Penichet ML, Bekaii-Saab T. Immunogenicity and antitumor efficacy of a novel human PD-1 B-cell vaccine (PD1-Vaxx) and combination immunotherapy with dual trastuzumab/pertuzumab-like HER-2 B-cell epitope vaccines (B-Vaxx) in a syngeneic mouse model. *Oncoimmunology*. 2020;9(1):1818437. doi:10.1080/2162402X.2020.1818437.
13. Garrett JT, Rawale S, Allen SD, Phillips G, Forni G, Morris JC, Kaumaya PTP. Novel engineered trastuzumab conformational epitopes demonstrate in vitro and in vivo antitumor properties against HER-2/ neu. *J Immunol*. 2007;178(11):7120–7131. doi:10.4049/jimmunol.178.11.7120.
14. Allen SD, Garrett JT, Rawale SV, Jones AL, Phillips G, Forni G, Morris JC, Oshima RG, Kaumaya PTP. Peptide Vaccines of the HER-2/ neu dimerization loop are effective in inhibiting mammary tumor growth in vivo. *J Immunol*. 2007;179(1):472–482. doi:10.4049/jimmunol.179.1.472.
15. Bekaii-Saab T, Wesolowski R, Ahn DH, Wu C, Mortazavi A, Lustberg M, Ramaswamy B, Fowler J, Wei L, Overholser J. Phase I immunotherapy trial with two chimeric HER-2 B-cell peptide vaccines emulsified in montanide ISA 720VG and Nor-MDP adjuvant in patients with advanced solid tumors. *Clin Cancer Res*. 2019;25(12):3495–3507. doi:10.1158/1078-0432.CCR-18-3997.
16. Guo L, Overholser J, Good AJ, Ede NJ, Kaumaya PTP. Preclinical studies of a novel human PD-1 B-cell peptide cancer vaccine PD1-vaxx from BALB/c mice to beagle dogs and to non-human primates (Cynomolgus monkeys). *Front Oncol*. 2022;12:826566. doi:10.3389/fonc.2022.826566.
17. Foy KC, Miller MJ, Moldovan N, Carson WE, Kaumaya PTP. Combined vaccination with HER-2 peptide followed by therapy with VEGF peptide mimics exerts effective anti-tumor and anti-angiogenic effects in vitro and in vivo. *Oncoimmunology*. 2012;1(7):1048–1060. doi:10.4161/onci.20708.
18. Wei WZ, Shi WP, Galy A, Lichlyter D, Hernandez S, Groner B, Heilbrun L, Jones RF. Protection against mammary tumor growth by vaccination with full-length, modified human ErbB-2 DNA. *Int J Cancer*. 1999;81(5):748–754. doi:10.1002/(SICI)1097-0215(19990531)81:5<748::AID-IJC14>3.0.CO;2-6.
19. Robbins PF, Kantor JA, Salgaller M, Hand PH, Fernsten PD, Schlom J. Transduction and expression of the human carcinoembryonic antigen gene in a murine colon carcinoma cell line. *Cancer Res*. 1991;51:3657–3662.
20. Kumar P, Nagarajan A, Uchil PD. Analysis of Cell Viability by the MTT Assay. *Cold Spring Harb Protoc*. 2018 Jun 1;2018(6). doi: 10.1101/pdb.prot095505. PMID: 29858338.
21. K-cs KPTP, DiGeorge AM, Stevens V. PEPTIDES. In Basava Anantharamaiah GM, editors. Boston, US: pringer-Verlag; 1994: 133–164
22. Lee HT, Lee JY, Lim H, Lee SH, Moon YJ, Pyo HJ, Ryu SE, Shin W, Heo Y-S. Molecular mechanism of PD-1/PD-L1 blockade via anti-PD-L1 antibodies atezolizumab and durvalumab. *Sci Rep*. 2017;7(1):5532. doi:10.1038/s41598-017-06002-8.
23. Zhang F, Qi X, Wang X, Wei D, Wu J, Feng L, Cai H, Wang Y, Zeng N, Xu T. Structural basis of the therapeutic anti-PD-L1 antibody atezolizumab. *Oncotarget*. 2017;8(52):90215–90224. doi:10.18632/oncotarget.21652.
24. Zak KM, Kitel R, Przetocka S, Golik P, Guzik K, Musielak B, Dömling A, Dubin G, Holak TA. Structure of the Complex of Human Programmed Death 1, PD-1, and Its Ligand PD-L1. *Structure*. 2015;23(12):2341–2348. doi:10.1016/j.str.2015.09.010.
25. Lin DY, Tanaka Y, Iwasaki M, Gittis AG, Su H-P, Mikami B, Okazaki T, Honjo T, Minato N, Garboczi DN. The PD-1/PD-L1 complex resembles the antigen-binding Fv domains of antibodies and T cell receptors. *Proc Natl Acad Sci U S A*. 2008;105(8):3011–3016. doi:10.1073/pnas.0712278105.
26. Liu Z, Wang H, Hu C, Wu C, Wang J, Hu F, Fu Y, Wen J, Zhang W. Targeting autophagy enhances atezolizumab-induced mitochondria-related apoptosis in osteosarcoma. *Cell Death & Disease*. 2021;12(2):164. doi:10.1038/s41419-021-03449-6.
27. Zhang L, Chen Y, Li F, Bao L, Liu W. Atezolizumab and bevacizumab attenuate cisplatin resistant ovarian cancer cells progression synergistically via suppressing epithelial-mesenchymal transition. *Front Immunol*. 2019;10:867. doi:10.3389/fimmu.2019.00867.
28. Boyerinas B, Jochems C, Fantini M, Heery CR, Gulley JL, Tsang KY, Schlom J. Antibody-dependent cellular cytotoxicity activity of a novel Anti-PD-L1 antibody avelumab (MSB0010718C) on human tumor cells. *Cancer Immunol Res*. 2015;3(10):1148–1157. doi:10.1158/2326-6066.CIR-15-0059.
29. Jochems C, Hodge JW, Fantini M, Tsang KY, Vandever AJ, Gulley JL, Schlom J. ADCC employing an NK cell line (haNK) expressing the high affinity CD16 allele with avelumab, an anti-PD-L1 antibody. *Int J Cancer*. 2017;141(3):583–593. doi:10.1002/ijc.30767.
30. Park JE, Kim SE, Keam B. Anti-tumor effects of NK cells and anti-PD-L1 antibody with antibody-dependent cellular cytotoxicity in PD-L1-positive cancer cell lines. *J Immunother Cancer*. 2020;8(2):e000873. doi:10.1136/jitc-2020-000873.
31. Guo L, Kaumaya PTP. First prototype checkpoint inhibitor B-cell epitope vaccine (PD1-Vaxx) en route to human Phase I clinical trial in Australia and USA: exploiting future novel synergistic vaccine combinations. *British Journal of Cancer*. 2021;125(2):152–154. doi:10.1038/s41416-021-01342-9.
32. Kaumaya PT. B-cell epitope peptide cancer vaccines: a new paradigm for combination immunotherapies with novel checkpoint peptide vaccine. *Future Oncol*. 2020;16(23):1767–1791. doi:10.2217/fon-2020-0224.
33. Tobias J, Steinberger P, Drinić M, Wiedermann U. Emerging targets for anticancer vaccination: PD-1. *ESMO Open*. 2021;6(5):100278. doi:10.1016/j.esmoop.2021.100278.
34. Shaabani S, Huizinga HPS, Butera R. A patent review on PD-1/PD-L1 antagonists: small molecules, peptides, and macrocycles (2015-2018). *Expert Opin Ther Pat*. 2018;28(9):665–678. doi:10.1080/13543776.2018.1512706.
35. Zarganes-Tzitzikas T, Konstantinidou M, Gao Y, Krzemien D, Zak K, Dubin G, Holak TA, Dömling A. Inhibitors of programmed cell death 1 (PD-1): a patent review (2010-2015). *Expert Opin Ther Pat*. 2016;26(9):973–977. doi:10.1080/13543776.2016.1206527.
36. Zhan MM, Hu XQ, Liu XX, Ruan B-F, Xu J, Liao C. From monoclonal antibodies to small molecules: the development of inhibitors targeting the PD-1/PD-L1 pathway. *Drug Discov Today*. 2016;21(6):1027–1036. doi:10.1016/j.drudis.2016.04.011.
37. Sasikumar PG, Sudarshan NS, Adurthi S. PD-1 derived CA-170 is an oral immune checkpoint inhibitor that exhibits preclinical anti-tumor efficacy. *Commun Biol*. 2021;4(1):699. doi:10.1038/s42003-021-02191-1.
38. Okazaki T, Chikuma S, Iwai Y, Fagarasan S, Honjo T. A. A rheostat for immune responses: the unique properties of PD-1 and their advantages for clinical application. *Nat Immunol*. 2013;14(12):1212–1218. doi:10.1038/ni.2762.
39. Flies DB, Sandler BJ, Sznol M, Chen L. Blockade of the B7-H1/PD-1 pathway for cancer immunotherapy. *Yale J Biol Med*. 2011;84(4):409–421.
40. Tian H, Kang Y, Song X, Xu Y, Chen H, Gong X, Zhang W, Xu Y, Xia X, Gao X, et al. PDL1-targeted vaccine exhibits potent

- antitumor activity by simultaneously blocking PD1/PDL1 pathway and activating PDL1-specific immune responses. *Cancer Lett.* **2020**;476:170–182. doi:[10.1016/j.canlet.2020.02.024](https://doi.org/10.1016/j.canlet.2020.02.024).
41. Lin Z, Zhang Y, Cai H, Zhou F, Gao H, Deng L, Li R. A PD-L1-based cancer vaccine elicits antitumor immunity in a mouse melanoma model. *Mol Ther Oncolytics.* **2019**;14:222–232. doi:[10.1016/j.omto.2019.06.002](https://doi.org/10.1016/j.omto.2019.06.002).
42. Sundaram R, Lynch MP, Rawale SV, Sun Y, Kazanji M, Kaumaya PTP. De novo design of peptide immunogens that mimic the coiled coil region of human T-cell leukemia virus type-1 glycoprotein 21 transmembrane subunit for induction of native protein reactive neutralizing antibodies. *J Biol Chem.* **2004**;279(23):24141–24151. doi:[10.1074/jbc.M313210200](https://doi.org/10.1074/jbc.M313210200).
43. Chen YL, Cui Y, Liu X, Liu G, Dong X, Tang L, Hung Y, Wang C, Feng M-Q. A bispecific antibody targeting HER2 and PD-L1 inhibits tumor growth with superior efficacy. *J Biol Chem.* **2021**;297(6):101420. doi:[10.1016/j.jbc.2021.101420](https://doi.org/10.1016/j.jbc.2021.101420).
44. Gu CL, Zhu HX, Deng L, Meng X-Q, Li K, Xu W, Zhao L, Liu Y-Q, Zhu Z-P, Huang H-M. Bispecific antibody simultaneously targeting PD1 and HER2 inhibits tumor growth via direct tumor cell killing in combination with PD1/PDL1 blockade and HER2 inhibition. *Acta Pharmacol Sin.* **2022**;43(3):672–680. doi:[10.1038/s41401-021-00683-8](https://doi.org/10.1038/s41401-021-00683-8).